Supplementary Information (SI)

Coarse-grained molecular dynamics simulations of nanoplastics interacting with a hydrophobic environment in aqueous solution

Lorenz F. Dettmann[a], Oliver Kühn[ab], and Ashour A. Ahmed[ab*]

[a] *University of Rostock, Institute of Physics, Albert-Einstein-Str. 23-24, D-18059 Rostock, Germany. E-mail: ashour.ahmed@uni-rostock.de*
[b] *University of Rostock, Department of Life, Light and Matter (LLM), Albert-Einstein-Str. 25, D-18059 Rostock, Germany*

I. Diffusion of coarse-grained water through CNTs

The goal of this investigation was to find a suitable CNT structure for studying interactions and movements of polymers inside and outside the CNT. Therefore, the corresponding water particles in presence of the CNT should have a relatively constant diffusion to make the movement of the NPs smooth. The movement of the water particles was investigated by calculating their mean-squared-displacements (MSDs):

$$\langle \Delta \mathbf{r}(t)^2 \rangle = \frac{1}{N} \sum_{i=1}^{N} (\mathbf{r}_i(t) - \mathbf{r}_i(0))^2 \tag{1}$$

A relatively congruent and constant rise of the calculated MSDs for the water inside a CNT indicates a constant diffusion of the water particles. The whole set of the CNTs had three different diameters: 15 Å, 20 Å and 30 Å. Furthermore for each diameter, three different lengths were used: 50 Å, 100 Å and 125 Å. In total, this results in nine CNT models. Each model is marked with one number (see Tab. S1) . Periodic boundary conditions were applied in each Cartesian dimension. The initial box dimensions were designed so that the tubes have a distance of 50 Å in x- and y-direction and at least 50 Å in z-direction to their periodic image. The boxes were filled with water which had an initial density of approximately 1 g cm^{-3}.
First, for every system, an energy minimization was performed. With the resulting structures, an NPT simulation for 100 ns was done, to adjust the box dimensions. Finally, for each system, the MSD was calculated by an NVT simulation, with a simulation time of 500 ns. The box dimensions of the NPT simulations were averaged over the whole time and applied to the NVT systems. MSDs of water particles inside the CNTs were calculated using the VMD RMSD tool [1]. For water, an antifreeze particle concentration of $AF = 15\,\%$ was applied. This concentration was sufficient to prevent the freezing of water in most of the models. Due to the antifreeze particles, the density of the systems changed to around 0.86 g cm^{-3} after equilibration.

Since the MSD can just be calculated for a fixed particle selection, one has to make sure that only water in the inner region is included into the analysis. Therefore, the following procedure was applied: First, one chooses a snapshot of the trajectory and selects a random unbiased set of water particles in the middle of the inner CNT, for this snapshot. This selection is restricted in a volume that goes 5 Å in the positive and negative z-direction from the middle of the CNT and to its inner walls (see Fig. S1). Then, from the chosen snapshot on, one observes the trajectory. Thereby, the selection of water particles is moving inside the CNT, until one of the particles is going to leave the CNT. This new snapshot would mark the end of the analysis interval. For the resulting time span, the MSD is calculated just for this selection. For one CNT, this analysis is repeated six times, starting at six different snapshots of the corresponding NVT trajectory. It has to be noted that due to the random choice and the different diameters of the CNT that the number of particles in the selection is varying. The resulting MSDs are shown in Fig. S2. Furthermore, the MSD of bulk water is plotted in every diagram (black line). The individual calculated curves for one CNT should be similar as possible, to indicate a relatively constant diffusion of the water particles.

In overall, the fluctuations of the MSDs are strong, compared to the MSD for bulk water. The main reason for this might be the relatively low number of water particles used for the calculation. Model 8 and 9 show sufficient congruence between the individual MSDs, as well as a relatively constant rise. Finally, after considering these two models, the CNT of model 8 was chosen for the investigation with NPs, because it would require a smaller simulation box, due to its smaller length.

Table S1: Detailed Information about the model systems, with d and l being the diameter and the length of the CNT, followed by the box dimensions. The other columns denote the number of water particles N_w, number of carbon atoms in the atomistic representation N_C(AT), number of beads in the coarse-grained (CG) system N_b(CG), number of rings of the CNT N_R(CG) and the ring size Rs(CG) (how many beads in one ring). The bond length between two beads equals to 4.7 Å.

model	d [Å]	l [Å]	Box [Å^3]	N_W	N_C(AT)	N_b(CG)	N_R(CG)	Rs(CG)
1	15	50	65×65×175	5960	960	130	13	10
2	15	100	65×65×175	5960	1920	260	26	10
3	15	125	65×65×175	5960	2400	320	32	10
4	20	50	70×70×175	6900	1248	182	13	14
5	20	100	70×70×175	6900	2496	364	26	14
6	20	125	70×70×175	6900	3120	448	32	14
7	30	50	80×80×175	9100	1872	260	13	20
8	30	100	80×80×175	9100	3744	520	26	20
9	30	125	80×80×175	9100	4680	640	32	20

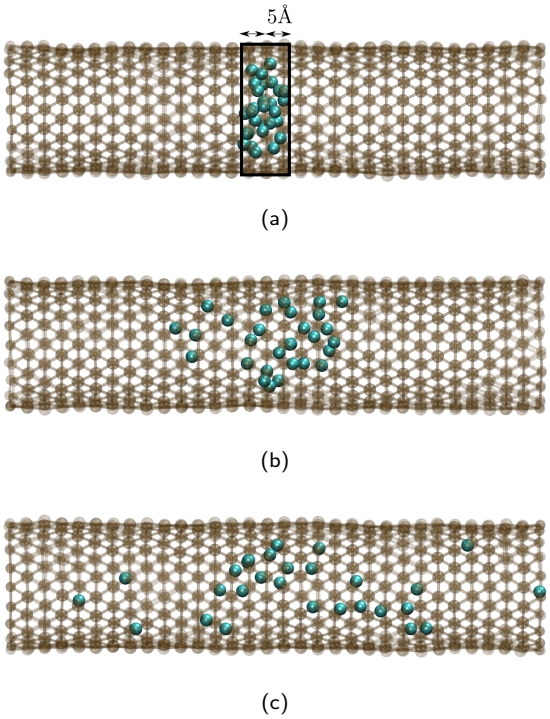

Fig. S1: Visualization of a certain selection of water particles and their time evolution for model 9. From such a trajectory, one MSD is calculated for the corresponding CNT for six different starting configurations. Picture (a) shows the trajectory after 0 ns, picture (b) after 0.18 ns and picture (c) after 3.56 ns of the analysis interval.

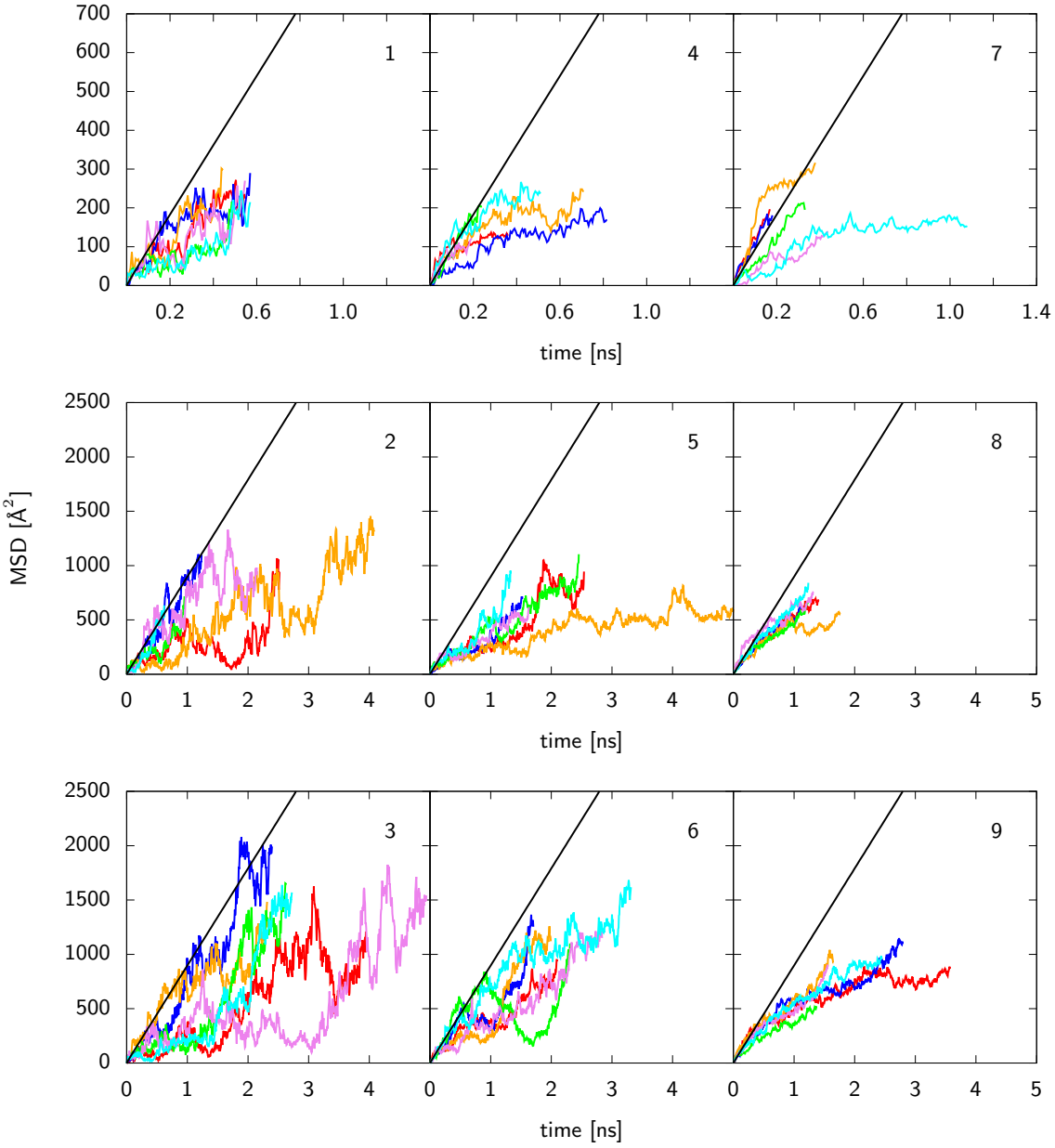

Fig. S2: MSD curves for the models 1 to 9. In each system, the MSD was calculated six times, resulting in six MSDs with the colors blue, red, orange, cyan, green, and violet. The black lines represent the MSD of bulk water from a separate model system.

II. Interaction energies and radial distribution functions between NPs and water

Table S2: Information about the individual polymer types regarding their CG representation. Bond lengths relate to the equilibrium distance between two neighboring beads. For PS the bond length applies to every bond of the polymer. The bead names and their corresponding LJ parameters are defined in the MARTINI force field. The beads consist of the listed atoms. One phenyl ring of PS is represented by three STY beads, which are identical.

Polymer	PEO	PE	PP	PS
Bond length	0.322 nm (EO-EO), 0.280 nm (SP2-EO)	0.460 nm	0.298 nm	0.270 nm
Bead names	SP2, EO	C1	SC1	STY, SCY
Atoms	$OHCH_2$, CH_2OCH_2	$4\times CH_2$	CH_2CHCH_3	CHC(H), CH_2CH
Mass in u (1 Bead)	31, 44	56	42	26, 27

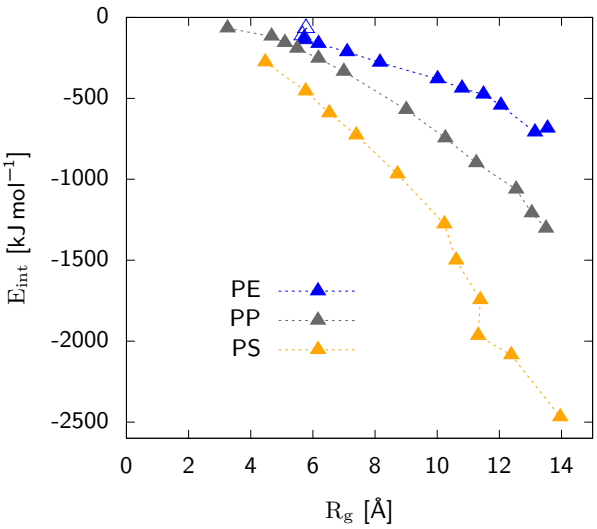

Fig. S3: Interaction energy between NPs and water depending on their average R_g.

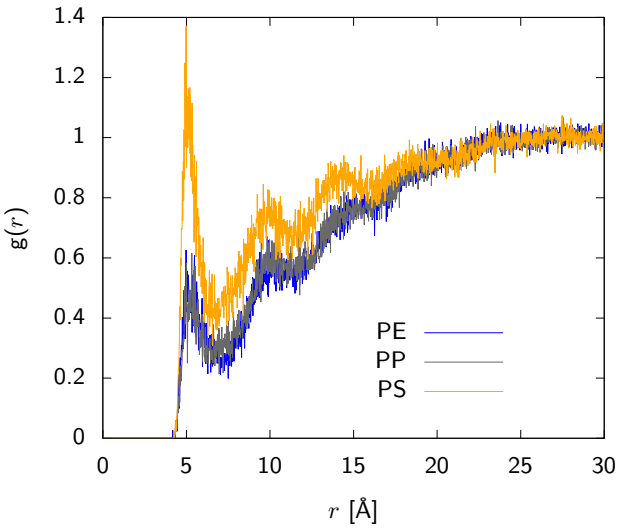

Fig. S4: Radial distribution function (RDF) of water to NPs, having an R_g of around 10 Å. For calculating the RDFs, one bead was selected at the surface of each NP particle.

From Fig. S3, we conclude that PS has the lowest hydrophobicity compared to PE and PP, due to the relatively strong interaction with water. A similar result is given by the high peak of the RDF for PS to water, shown in Fig. S4. However, it should be noted that the CG potential for PS is not retaining its tacticity, so that the phenyl groups can move freely around the alkane chain. It was therefore observed, that the phenyl groups are mostly located towards water. This effect might underestimate the hydrophobicity of PS.

III. Coarse-grained vs. atomistic representation of polymers in water

To validate the present modeling approach and especially related to Section 3.1 "NPs in water", we performed in total additional 12 atomistic molecular dynamics (MD) simulations. Specifically, all the four polymers (PE, PEO, PP and PS) were considered with three different chain lengths for each involving 10, 45 and 100 monomer units. Each MD simulation involved one polymer inside a box containing simple point charge (SPC) water molecules with a density of about $1\,\mathrm{g\,cm^{-3}}$. Periodic boundary conditions were applied in all directions. For all MD simulations, an energy minimization was carried out followed by two equilibration runs using canonical (NVT) and isothermal-isobaric (NPT) ensembles at 300 K. Then, a subsequent production MD run of about 20 ns was performed for each case with a time step of 2 fs. All calculations were performed using the GROMACS software package [2–4] combined with the general CHARMM force field [5, 6].

The production MD trajectories were analyzed and mainly the averaged radius of gyration of each polymer and interaction energy between each polymer and water were considered, here for testing the present CG models versus the corresponding atomistic models. The CG and atomistic results were compiled into Figs. S5 and S6 and Tables S3 and S4. In general, the results refer to a good agreement between the CG and atomistic representations. Specifically, the radii of gyration obtained by CG show the same trend obtained by the relatively more accurate representation (i.e., atomistic simulation) with a correlation having a determination of coefficient (R^2) of 0.991 (see Fig. S5). Moreover, the CG representation shows a good correlation with the atomistic one ($R^2 = 0.949$) for the interaction energy values. This agreement between the results of both CG and atomistic representations refers to the validity and ability of the CG approach to simulate the present molecular models and especially NPs in water.

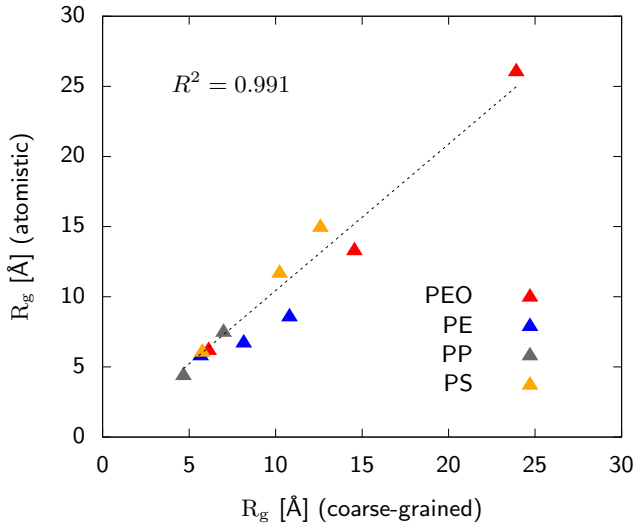

Fig. S5: Comparison of radii of gyration of NPs in water between coarse-grained and atomistic representation.

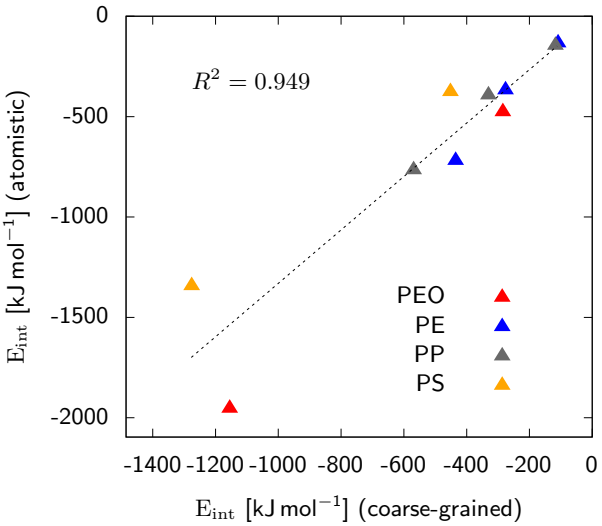

Fig. S6: Comparison of interaction energies of NPs with water, between coarse-grained and atomistic representation.

Table S3: Radius of gyration for NPs in water for different number of monomers N for CG and atomistic (AT) representation. Values denoted with * were estimated by the fitting curve, given in Fig. 2 of the main manuscript.

R_g [Å]	PEO		PE		PP		PS	
N	CG	AT	CG	AT	CG	AT	CG	AT
10	6.13	6.15	5.67	5.77	4.67	4.36	5.77	6.03
45	14.56	14.83	8.16	6.68	6.99	7.45	10.23	11.66
100	23.91*	26.03	10.80	8.55	9.00	9.74	12.59*	14.38

Table S4: Interaction energies between NPs and water for different number of monomers N for CG and AT representation.

E_{int} [kJ mol^{-1}]	PEO		PE		PP		PS	
N	CG	AT	CG	AT	CG	AT	CG	AT
10	-287.9	-477.0	-111.8	-133.9	-117.2	-146.4	-455.4	-376.6
45	-1156.2	-1953.9	-278.1	-368.2	-334.3	-393.3	-1277.4	-1343.1
100	-	-4317.9	-438.2	-719.6	-570.4	-765.7	-	-2079.4

IV. Snapshots for PE and interaction energies for PP & PS

Additional information about the starting configurations for the models with polymers placed outside the CNT can be summarized as follows: Some polymers did not interact with the CNT. In such cases, the simulation is repeated with slightly different starting configurations or continued, until an interaction is observed. So, the first starting configuration can vary. Also, if e.g. the polymer adsorbs too fast at the outer wall, the time window for recording the interaction energy in solution may be too short, which might result in a larger error for the calculated energy, compared to a longer solution phase period. In such a case, the simulation is repeated with the only change that the polymer is placed more far away from the outer wall of the CNT (e.g. with a distance of 40 Å). It was also observed that a polymer initially placed in solution was going inside the CNT during the simulation. Then, the simulation is repeated with a higher distance to the CNT. The course of the simulations is strongly depending on the starting conditions, e.g. the initial velocities of the water particles. Relevant for this investigation are the time intervals in the simulations, when the polymers are in bulk water, adsorbed at the outer wall or inside the CNT. These time intervals should be relatively large, so that the calculated interaction energies have a lower error.

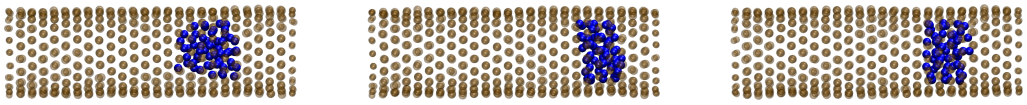

(a) (b) (c)

Fig. S7: Snapshots from the NVT simulation with PE initially placed inside the CNT (R_g = 9 Å). (a) shows the initial position, (b) the trajectory after 250 ns and (c) the trajectory after 500 ns. PE doesn't leave the CNT, indicating a generally high stability of adsorbed configurations.

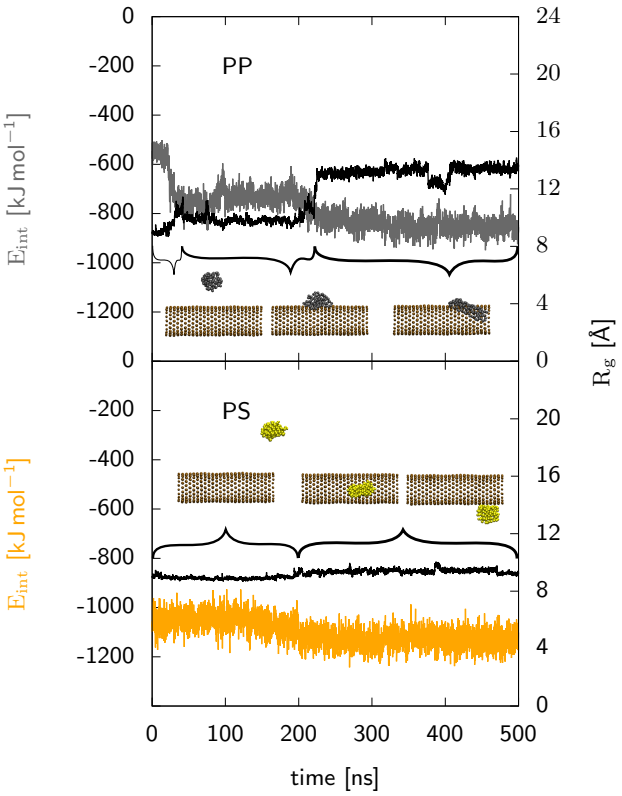

Fig. S8: Interaction energies in the course of the NVT simulations for PP (gray) and PS (orange) with initially R_g = 9 Å. For both polymers, the lines relate to the simulations with the polymer chains outside the CNT. The interaction energy between the respective chain and the rest of the system is considered. Furthermore, R_g (black) is plotted for both polymer types.

V. Lateral position densities and radii of gyration for PEO & PS inside the CNTs

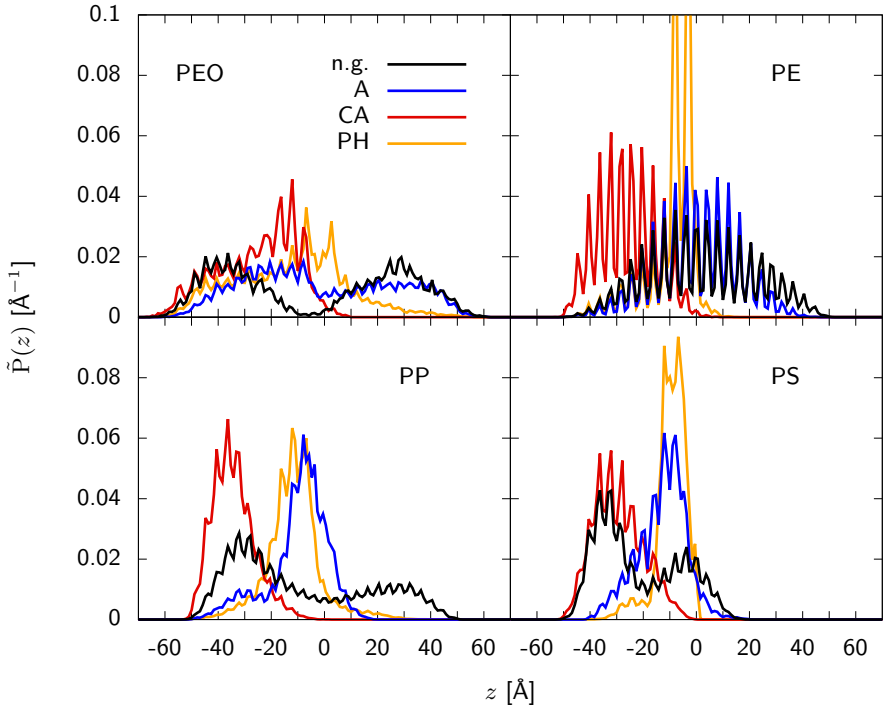

Fig. S9: Normalized partial densities, $\tilde{P}(z)$, for different polymers being (mostly) inside the CNT ($-50\,\text{Å} < z < 50\,\text{Å}$), depending on their position z. Here, densities are not symmetrized, like in Fig. 5 of the main text. $z = 0$ denotes the center of mass of the CNT, or rather the position of functional groups, if present. The polymers starting configurations were in the range of negative z values. In these diagrams one can see that in some cases of present functional groups, it is possible that the polymer penetrates into the range of positive z values (e.g. PEO-A, or PE-A). Note that for PE-PH the two maxima which are out of the scale reach $\sim 0.16\,\text{Å}^{-1}$.

For the functional groups, the particle/bead C1 from the MARTINI force field was used for alkane chains, P3 for carboxylic acid groups and SC5 for phenyl groups.

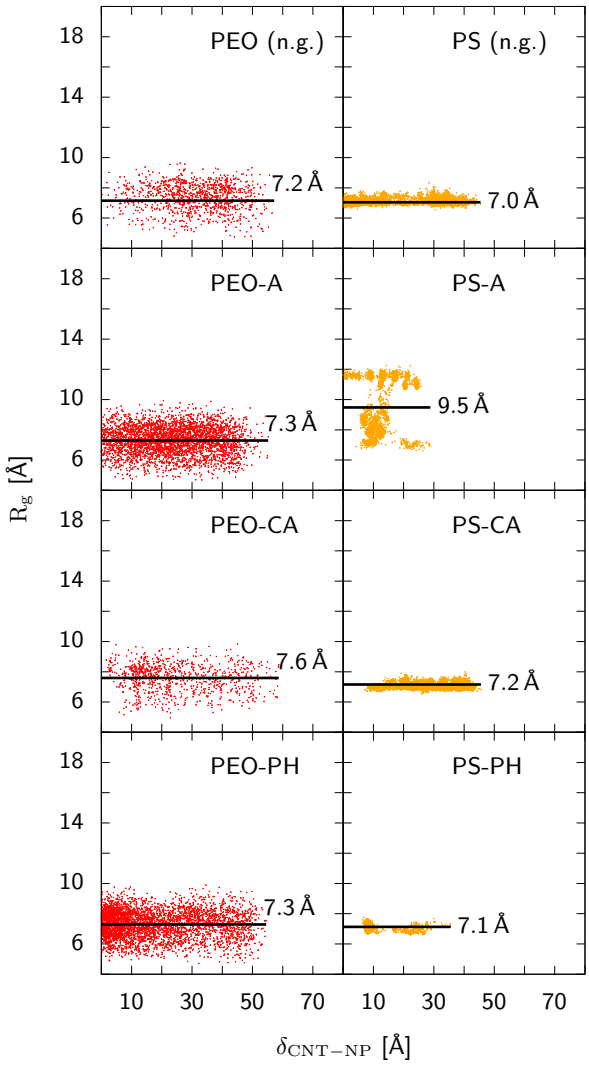

Fig. S10: R_g of polymer chains inside the CNT, depending on the center of mass distance δ_{CNT-P} between the respective polymer and the CNT. Colors red and orange relate to the polymer types PEO and PS, respectively. The radius of gyration for PEO is not significantly influenced by present functional groups, visible in the very similar distributions of R_g. Only the sample density (number of data points) for the cases with bare CNT and attached carboxylic acid groups is smaller, because the polymer left the CNT at earlier times. PS on the other hand shows a higher distribution for the case with alkane chains, due to an unfolding of the polymer. In all the other models, R_g remains relatively constant, underlining the rigidity of PS.

VI. Ring structure in the case of PE-PH

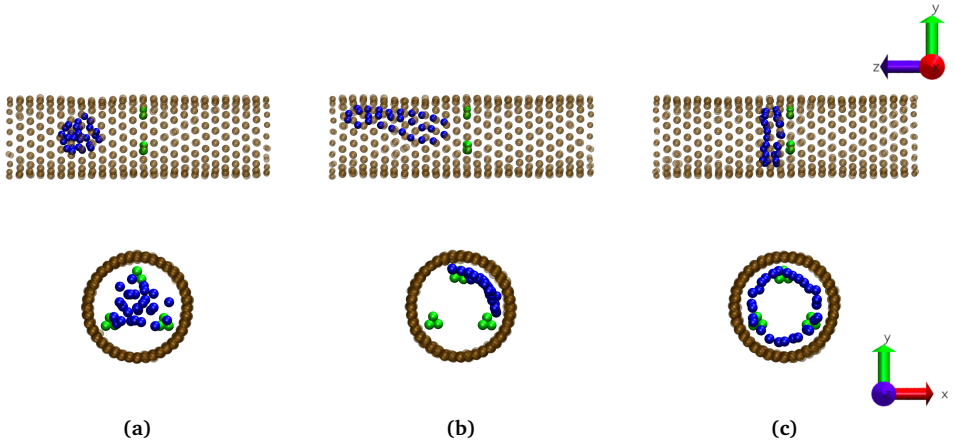

Fig. S11: Snapshots from the NVT simulation of PE (blue) being inside the CNT (brown) with phenyl groups (green). Two pictures in one figure correspond to the side and front view on the system. (a) shows the initial position, (b) shows the trajectory after 100 ns, and (c) the trajectory after 308 ns. In this simulation, PE folds itself to a ring structure right next to the phenyl groups. For a better visualization, water particles are left out.

References

[1] W. Humphrey, A. Dalke, and K. Schulten. VMD: Visual molecular dynamics. *Journal of Molecular Graphics*, 14(1):33–38, February 1996.

[2] B. Hess, C. Kutzner, D. van der Spoel, and E. Lindahl. GROMACS 4: algorithms for highly efficient, load-balanced, and scalable molecular simulation. *Journal of Chemical Theory and Computation*, 4(3):435–447, February 2008.

[3] M. J. Abraham, T. Murtola, R. Schulz, S. Páll, J. C. Smith, B. Hess, and E. Lindahl. GROMACS: High performance molecular simulations through multi-level parallelism from laptops to supercomputers. *SoftwareX*, 1-2:19–25, September 2015.

[4] E. Lindahl, M. J. Abraham, B. Hess, and D. van der Spoel. Gromacs 2019.4 source code, 2019.

[5] J. Lee, X. Cheng, J. M. Swails, M. S. Yeom, P. K. Eastman, J. A. Lemkul, S. Wei, J. Buckner, J. C. Jeong, Y. Qi, S. Jo, V. S. Pande, D. A. Case, C. L. Brooks, A. D. MacKerell, J. B. Klauda, and W. Im. CHARMM-GUI input generator for NAMD, GROMACS, AMBER, OpenMM, and CHARMM/OpenMM simulations using the CHARMM36 additive force field. *Journal of Chemical Theory and Computation*, 12(1):405–413, December 2015.

[6] K. Vanommeslaeghe, E. Hatcher, C. Acharya, S. Kundu, S. Zhong, J. Shim, E. Darian, O. Guvench, P. Lopes, I. Vorobyov, and A. D. Mackerell. CHARMM general force field: A force field for drug-like molecules compatible with the CHARMM all-atom additive biological force fields. *Journal of Computational Chemistry*, pages NA–NA, 2009.